Supplementary information

Antibiotic-resistant bacteria show widespread collateral sensitivity to antimicrobial peptides

Viktória Lázár[1,#,§], Ana Martins[1,#], Réka Spohn[1], Lejla Daruka[1], Gábor Grézal[1], Gergely Fekete[1], Mónika Számel[1], Pramod K Jangir[1], Bálint Kintses[1], Bálint Csörgő[1], Ákos Nyerges[1], Ádám Györkei[1], András Kincses[2], András Dér[2], Fruzsina R Walter[3], Mária A Deli[3], Edit Urbán[4] Zsófia Hegedűs[5], Gábor Olajos[5], Orsolya Méhi[1], Balázs Bálint[6], István Nagy[6,7], Tamás A Martinek[5], Balázs Papp[1,*], Csaba Pál[1,*]

[1]Synthetic and Systems Biology Unit, Institute of Biochemistry, Biological Research Centre, Hungarian Academy of Sciences, Szeged, Hungary
[2]Biomolecular Electronics Research Group, Bionanoscience Unit, Institute of Biophysics, Biological Research Centre, Hungarian Academy of Sciences, Szeged, Hungary
[3]Biological Barriers Research Group, Institute of Biophysics, Biological Research Centre, Hungarian Academy of Sciences, Szeged, Hungary
[4]Institute of Clinical Microbiology, Albert Szent-Györgyi Medical and Pharmaceutical Center, Faculty of Medicine, University of Szeged, Szeged, Hungary
[5]Institute of Pharmaceutical Analysis, University of Szeged, Szeged, Hungary
[6]SeqOmics Biotechnology Ltd., Mórahalom, Hungary
[7]Sequencing Platform, Institute of Biochemistry, Biological Research Centre of the Hungarian Academy of Sciences, Szeged, Hungary

[§]Current Affiliation: Faculty of Biology, Technion - Israel Institute of Technology, Haifa, Israel.

[#]The authors contributed equally to this work.

*Correspondence should be sent to: Csaba Pál (cpal@brc.hu) or Balázs Papp (pappb@brc.hu)
Synthetic and Systems Biology Unit, Institute of Biochemistry, Biological Research Centre, Temesvári krt 62, Szeged 6726,
Hungary. Tel.: +36 62 599 661; Fax: +36 62 433 506

Table of contents

Supplementary Texts

Supplementary Text 1 – Role of *sbmA* and *marR* genes in cross-resistance and collateral sensitivity to antimicrobial peptides in a laboratory and a clinical *E. coli* background

The *sbmA* and *marR* genes play a key role in the observed cross-resistance (CR) and collateral sensitivity (CS) patterns of antibiotic-resistant strains towards antimicrobial peptides (Table 1, main text). Deletion of *sbmA* is an important contributor to the cross-resistance of aminoglycoside-resistant strains to the proline-rich P2 peptides, while the Val84Glu mutation of *marR* yields widespread collateral sensitivity to P3 peptides (Table 1, main text). To evaluate whether these mutations contribute to CS and CR when they are present in a pathogenic bacterial background, we inserted these two mutations into the antibiotic-sensitive clinical isolate *E. coli* ATCC 25922, a strain used as a standard control for antibiotic susceptibility in clinical laboratories.

Results in *E. coli* ATCC 25922 and *E. coli* BW25113 fully agree. As expected, deletion of *sbmA* in the clinical isolate *E. coli* ATCC 25922 provides resistance to aminoglycosides tobramycin (TOB) and kanamycin (KAN), while simultaneously confers cross-resistance to the proline-rich P2 peptides Bactenecin 5 (BAC5) and Apidaecin IB (AP) (Supplementary Figure 4A-D). Moreover, this mutation caused increased sensitivity towards P3 peptides indolicidin (IND) and human beta defensin 3(HBD3) in both strains (Supplementary Figure 4E-F and Table 1).

In a similar way, the phenotypic effects of the mutation Val84Glu in the *marR* gene are very similar in the two *E. coli* strains. It results in increased resistance to various antibiotics, including tetracycline (TET) and chloramphenicol (CHL), while the same mutation causes collateral sensitivity to P3 peptides, such as HBD3 and CAP18 (Supplementary Figure 4G-J).

Supplementary Text 2 - Potential mechanisms contributing to cross-resistance between aminoglycosides and antimicrobial peptides

In addition to the mechanisms described in the main text, we noted that aminoglycoside-resistant strains uniquely accumulated mutations in a broad class of genes that reduced the membrane electrochemical potential, a pattern also observed in aminoglycoside-resistant clinical isolates[1]. This could be significant, as there are similarities in the cellular uptake mechanisms of aminoglycosides and proline-rich antimicrobial peptides[2]. By decreasing the electrical potential across the inner membrane (i.e by membrane depolarization), resistant bacteria reduce the cellular uptake of aminoglycosides and proline-rich peptides as well. To gain further support of this idea, we focused on a gene involved in K^+ uptake (*trkH*) that was repeatedly mutated in the aminoglycoside-resistant strains. A typical mutation was inserted into wild-type *E. coli*, resulting in a diminished membrane potential[1]. As a consequence, susceptibility to both aminoglycosides and 2 out of the 4 proline-rich antimicrobial peptides (P2) decreased (see details in Table 1).

Supplementary Text 3 - Potential mechanism of collateral sensitivity of *ompC* loss-of-function mutant to pore-forming peptides

The *ompC* loss-of-function mutation contributes to resistance to antibiotics via reducing the uptake of hydrophilic antibiotics[3,4], but simultaneously enhances susceptibility to antimicrobial peptides, mainly those belonging to P2 and P3 groups (Table 1). What can be the mechanism leading to sensitivity to antimicrobial peptides? It has been established that under conditions that lead to outer membrane stress (such as detergents, metal ions and antimicrobial peptides), porins act as an upstream signal sensor that modulates *rpoE* activity[5-8]. *RpoE* is a sigma factor involved in maintaining the integrity of periplasmic and outer membrane components[8]. Specifically, *rpoE* and its targets such as the *degP* protease and genes involved in LPS biogenesis (*lpxD*, *lpxA*) play an important role in resistance to antimicrobial peptides[9-12]. Moreover, bacterial cells lacking porins or *rpoE* are sensitive to antimicrobial peptides and metal ions[7,8]. Based on these facts we hypothesized that the lack of *ompC* due to specific inactivating mutations leads to the reduction of the *rpoE* regulon-mediated response to membrane perturbations, which in turn results in enhanced susceptibility towards antimicrobial peptides. To test this hypothesis, two independent experiments were performed with an *ompC* loss-of-function mutant (see details in Table 1). First, we found that overexpression of *rpoE* diminishes collateral sensitivity of the ompC mutant towards peptides PGLA and HBD3 (Supplementary Figure 17). Moreover, we demonstrated that the *rpoE* dependent periplasmic protease, *degP* was significantly up-regulated after exposure to a sublethal level of the peptide PGLA in the wild-type strain, but not in the *ompC* mutant strain (Supplementary Figure 18). Taken together, these results indicate that a reduced *rpoE*-mediated outer membrane stress response following exposure to antimicrobial peptide underpins the collateral sensitivity of the *ompC* loss-of-function mutant strain to antimicrobial peptides.

Supplementary Text 4 – Drug cycling based on antibiotic and antimicrobial peptide combinations

Reciprocal collateral sensitivity is an emerging concept for the development of drug pairs that, in specific situations, may be useful to hinder resistance evolution via drug cycling in clinical conditions[13,14]. A prerequisite for the use of a drug cycling strategy is the reciprocal nature of the collateral sensitivity interaction, i.e. that resistance to drug A leads to sensitivity to drug B and *vice-versa*. To begin to investigate whether collateral sensitivity to antimicrobial peptides is reciprocal and therefore can be used for drug cycling, we generated and analyzed antimicrobial peptide resistant strains, as follows:

Laboratory evolution and phenotype profiling of antimicrobial peptide resistant strains

The purpose of this experiment was to demonstrate reciprocal collateral sensitivity between conventional antibiotics and antimicrobial peptides. We evolved 10 parallel populations of laboratory *E. coli* BW25113 towards the peptide CAP18 (Supplementary Method 2). CAP18 appears to be an ideal candidate for two reasons. First, numerous antibiotic-resistant strains exhibit collateral sensitivity against this peptide. Second, we found that evolution against this peptide readily occurs in the laboratory. More specifically, after only 130 generations, the 10 parallel lines reached as high as 256-657 increment in MIC level against CAP18 during the course of laboratory evolution.

Next, we isolated one strain from each of the five independently evolved populations with the highest CAP18 resistance level. We measured the susceptibility of these five CAP18-resistant strains towards 6 antibiotics, including tetracycline (TET), doxycycline (DOX), erythromycin (ERY), cefoxitin (FOX), nalidixic acid (NAL) and nitrofurantoin (NIT). We found that adaptation to CAP18 resulted in strong collateral sensitivity to four out of the six antibiotics tested (DOX, ERY, NAL and NIT). Strikingly, CAP18 resistant strains showed an up to 11-fold decrease in minimum inhibitory concentrations (Supplementary Figure 13).

Competition experiments

To investigate whether antibiotic-antimicrobial peptide pairs exhibiting reciprocal collateral sensitivity specifically inhibit the growth of resistant bacteria, we performed two competition experiments (Supplementary Method 3). We focused on nalidixic acid – CAP18 drug pairs. Nalidixic acid is an optimal candidate, as it is a bactericidal drug, and CAP18 resistant strains show an especially high sensitivity to nalidixic acid (Supplementary Figure 14). The NAL-resistant strains have accumulated mutations in an overlapping set of genes[1,15], and have very similar resistance and collateral sensitivity profiles to each other[1,15]. Therefore, we focused on a single, representative strain (NAL7) only.

In the first experiment, NAL7 and the wild-type were set to compete at various concentrations of CAP18. In the second experiment, a randomly selected CAP18-resistant strain (CAP18_5) and the wild-type were set to compete at various concentrations of Naldixic acid. In both cases, the strains were inoculated at an equal ratio at the start of the experiments. In both experiments 1 and 2, we identified a drug concentration range where the wild-type reached 100% frequency after as few as 18 hours of growth, and thereby outcompeted the resistant strain (Supplementary Figure 14). These results indicate that cyclical application of NAL and CAP18 may be feasible for the eradication of bacteria acquiring resistance to any of the two antimicrobials throughout the cycles.

Supplementary Methods

Supplementary Method 1- Promoter activity measurements

To measure changes in the promoter activity of *degP* in response to PGLA stress, we used a selected construct from a comprehensive GFP transcription reporter library[16] and transferred them into two different genetic backgrounds: the wild-type and the *ompC*[Met1Ile] mutant strains[16]. The reporter strain bears a low-copy plasmid with a promoter of interest controlling the expression of a fast folding GFP and carries a kanamycin resistance cassette. These plasmid-carrying strains were cultured overnight and optical densities were adjusted to OD_{600}=0.2. 100 µl of bacterial cultures were transferred to black 96-well microtiter plates and treated with three different PGLA concentrations (0, 1/2 and 4/5 of the MIC), in 4 replicates each. Plates were incubated in a Synergy 2 microplate reader at 30°C in medium supplemented with 50 µg/ml kanamycin. The OD and fluorescence curves were measured for 2h with 15s delays between readings. The first 15 data points were excluded from further analysis due to the high standard deviation between replicates. Data curves were smoothed and fluorescence per OD ratio curves were calculated. Next, areas under these ratio curves were determined. Finally, we calculated changes in GFP fluorescence intensity relative to the appropriate untreated controls derived from the same experiment.

Supplementary Method 2 - Experimental evolution of CAP18 resistance

Resistance to CAP18 was achieved by a previously established automated evolution experiment[17,18]. Starting with a subinhibitory CAP18 concentration, 10 parallel cultures were allowed to grow in Minimal salts medium (See Materials and Methods) at 30ºC degree. A chess-board layout was used on the plate to monitor potential cross-contamination events. After 24 hours of incubation, 20 µl of 350µl culture was transferred to four independent wells containing fresh medium and increasing dosages of CAP18 (0.5x, 1x, 1.5x and 2.5x the concentration of the previous step). Prior to each transfer, cell growth was monitored by measuring the optical density at 600 nm (OD_{600} value, Biotek Synergy 2 microplate reader was used for this purpose). Only populations with the highest drug concentration (and reaching OD_{600} > 0.2) were selected for further evolution. Accordingly, only one of the four populations was retained for each independently evolving lineage. This protocol was designed to avoid population extinction and to ensure that populations with the highest level of resistance were propagated further during evolution. Evolution lasted approximately 130 generations (20 transfers).

Supplementary Method 3 - Competition assay.

To evaluate whether antibiotic-antimicrobial peptide pairs exhibiting reciprocal collateral sensitivity inhibit the survival of resistant bacteria, we performed two competition experiments. In the first experiment, a NAL-resistant strain (NAL7) and the wild-type strain were competing in the presence of various concentrations of CAP18. The second experiment was vice-versa, *i.e.* a CAP18-resistant strain (CAP18_5) and the wild-type were competing under NAL stress. In both cases the initial ratio between the resistant and the wild-type strains was set to 1:1.

The wild-type (WT) and the investigated resistant strain (NAL7 or CAP18_5) were inoculated at an equal ratio with approximately 10^4 cells per genotype per mL in minimal salts medium. Parallel co-cultures were treated with various concentrations of CAP18 or NAL, respectively (3 biological replicates for each concentration and 3 biological replicates of untreated control co-cultures). At the beginning of the experiment (T0) as well as following 18 hours of incubation at 30°C with shaking (T18), serial dilutions were plated onto drug-free agar plates and agar plates supplemented with NAL (20µg/mL) or CAP18 (25 µg/mL), respectively. The drug-containing agar plates inhibited the growth of the wild-type, which allowed us to count the number of resistant colony forming units (CFU), while the number of total CFUs was counted on the drug-free agar plates. Viable colonies were counted after 24 hours of incubation on 30°C. The number of wild-type colonies was inferred by subtractring of the number of resistant CFUs from the number of total CFUs. To assure the accuracy of the results, T0 controls of both wild-type and resistant strains were plated both from co-cultures and alone onto both drug-free and drug-containing agar plates.

Supplementary Method 4 - pORTMAGE-based insertion of resistance-associated mutations

The previously described pORTMAGE[19] method was used to introduce antibiotic resistance-associated mutations in *Escherichia coli* ATCC 25922[20] and inactivate the *waaY* gene in *Escherichia coli* BW25113 wild-type, marR Val84Glu mutant (marR*), TET3, DOX3 and NAL7 strains. Briefly, individual mutations were introduced via synthetic ssDNA-mediated recombineering. These oligos were designed using MODEST[21], were 90 nucleotides long and had complementary sequences to the replicating lagging strand with a minimized secondary structure (≥-12 kcal/mol). Oligonucleotides were ordered from Integrated DNA Technologies (Coralville, IA, USA) with standard desalting. Recombineering was performed in the corresponding electrocompetent cells carrying pORTMAGE3 (Addgene plasmid ID: 72678). pORTMAGE3 was induced at 42°C for 15 minutes to allow for efficient mutation-incorporation and avoid off-target mutagenesis[19]. For each target strain 40 µl of induced electrocompetent cells were transformed with 1 µl of 100 µM mutation-carrying oligo. Cells were recovered in 5 ml Terrific-Broth (TB) media (24 g yeast extract, 12 g tryptone, 9.4 g K_2HPO_4, and 2 g KH_2PO_4 per 1 L of water) after electroporation and incubated at 30°C for 60 minutes, after which 5 ml Lysogeny-Broth-Lennox (LB^L) media (10 g tryptone, 5 g yeast extract, 5 g sodium chloride per 1 L water) was added and incubated at 30°C overnight. Cultures were then plated onto LB^L agar plates in appropriate dilutions to form individual colonies and incubated at 30°C overnight.

Colonies carrying the desired mutations were selected using either allele-specific colony-PCR or High Resolution Melting (HRM) analysis. Allele-specific colony-PCRs have been performed with DreamTaq Master Mix (Thermo Scientific) according to a standard protocol[19]. High-Resolution Melting (HRM) colony-PCRs have been performed with Luminaris HRM Master Mix (Thermo Scientific) in a Bio-Rad CFX96 qPCR machine according to the manufacturer's guidelines. Mutations were confirmed by capillary-sequencing. Finally, the pORTMAGE3 plasmid was removed from the sequence-verified colonies by growing the cells overnight at 42°C in antibiotic-

363 free LB^L media. Mutation-incorporating pORTMAGE oligonucleotides, allele-
364 specific colony-PCR, HRM PCR and sequencing primers are listed in
365 Supplementary Table 14.

366

Supplementary Method 5 – Surface charge measurements

Zeta potential measurement was performed on a Zetasizer Nano ZS instrument (Malvern Instruments), based on a previously established protocol, where changes in surface charge upon antimicrobial peptide treatment were measured in *Escherichia coli*[22]. Briefly, overnight grown bacteria were diluted in filtered phosphate-buffered saline (PBS) to reach a 10^6 cells/ml concentration and then washed (centrifuging at 3000 rpm for 10 mins at 4°C) and resuspended in filtered PBS. Bacterial samples were kept at 4°C until measurement. Upon measurement, samples were dispensed into disposable zeta cells with gold electrodes and allowed to equilibrate for 15 min at 25°C, before measuring at 25°C. Zeta potential was calculated from the measured electrophoretic mobility using the Smoluchowski approximation of the Henry equation[23]. Zeta potential was determined based on 8 technical and 5 biological replicates of both *marR* single-mutant and *waaY* overexpressing strains (the latter carried the *waaY* overexpression plasmid of the ASKA collection), and the respective controls (wild-type and wild-type containing the empty plasmid of the ASKA collection, respectively).

Supplementary Method 6 - High-throughput measurement of relative surface charge by a poly-L-lysine binding assay

To investigate changes in bacterial cell surface charge in a high-throughput manner (i.e. for dozens of strains), we performed a fluorescein isothiocyanate-labeled poly-L-lysine (Sigma) binding assay. Poly-L-lysine is a polycationic molecule that is widely used to study the interaction between cationic peptides and charged lipid bilayer membranes[24]. The binding assay was performed as described previously[25]. In brief, cells were grown overnight in minimal medium and then washed twice with 1X phosphate-buffered saline (PBS) buffer. The cells were suspended in the PBS buffer to a final OD_{600} of 0.1. The suspension was incubated with 6.5 μg ml^{-1} poly-L-lysine for 10 min and centrifuged 5500rpm for 5 min. The remaining amount of poly-L-lysine in the supernatant was determined fluorometrically (excitation at 500 nm and emission at 530 nm) without or with bacterial exposure. The quantity of bound molecules was calculated from the difference between these values. The lower the amount of bound poly-L-lysine, the less negatively charged the cell surface is.

Supplementary Tables

Supplementary Table 1 – Antibiotics employed and their modes of actions

Antibiotic	Abbreviation	Mode of action	Type of action
Ampicillin	AMP	Cell wall	Bactericidal
Cefoxitin	FOX	Cell wall	Bactericidal
Ciprofloxacin	CPR	Gyrase	Bactericidal
Nalidixic acid	NAL	Gyrase	Bactericidal
Nitrofurantoin	NIT	Multiple mechanisms	Bactericidal
Kanamycin	KAN	Protein synthesis, 30S, Aminoglycosides	Bactericidal
Tobramycin	TOB	Protein synthesis, 30S, Aminoglycosides	Bactericidal
Tetracycline	TET	Protein synthesis, 30S	Bacteriostatic
Doxycycline	DOX	Protein synthesis, 30S	Bacteriostatic
Chloramphenicol	CHL	Protein synthesis, 50S	Bacteriostatic
Erythromycin	ERY	Protein synthesis, 50S	Bacteriostatic
Trimethoprim	TRM	Folic acid biosynthesis	Bacteriostatic

Supplementary Table 2 – The list of antimicrobial peptides employed in this study and the available information about them based on literature mining

Provided in a separate Excel spreadsheet.

Supplementary Table 3 – Dataset of collateral sensitivity and cross-resistance interactions identified at the level of antibiotic-resistant strains

Provided in a separate Excel spreadsheet.

Supplementary Table 4 – Relative changes in the minimum inhibitory concentrations (MIC) of the antimicrobial peptides towards antibiotic-resistant strains

Provided in a separate Excel spreadsheet.

Supplementary Table 5 – Fraction of collateral sensitivity (blue) and cross-resistance (orange) interactions in each strain cluster (S1-4) for each peptide cluster (P1-3)

Collateral sensitivity dominates, especially in the case of the S3 strain cluster, in which marR mutations are enriched. The highest degree of collateral sensitivity is exhibited against the pore-forming P3 peptides ($p<0.0001$, Fisher's exact test). Cross-resistance of antibiotic-resistant bacteria to P2 peptides is frequent ($p<0.0001$, Fisher's exact test).

Fraction of Collateral Sensitivity

P3	P2	P1
0.46	0.18	0.05
0.17	0.06	0.01
0.6	0.19	0.17
0.67	0.02	0.28

Fraction of Cross-Resistance

	P3	P2	P1
S1	0.06	0.17	0
S2	0.26	0.31	0.18
S3	0.06	0.06	0.01
S4	0.06	0.69	0.02

Supplementary Table 6 – List of the main chemical and physical properties of the antimicrobial peptides employed in this study

Provided in a separate Excel spreadsheet.

Supplementary Table 7 – Susceptibility profiles of antibiotic-resistant *E. coli* clinical isolates across antimicrobial peptides

Provided in a separate Excel spreadsheet.

Supplementary Table 8 – Differential expression analysis of RNA-Seq data of 24 antibiotic-resistant strains

Provided in a separate Excel spreadsheet.

Supplementary Table 9 – Bile acid sensitivity of the antibiotic-resistant strains and list of genes involved in phospholipid and LPS synthesis

Provided in a separate Excel spreadsheet.

Supplementary Table 10 – List of genes sensitizing towards CAP18 and CP1 in the chemogenomic study

Provided in a separate Excel spreadsheet.

Supplementary Table 11 – Upregulation of LPS-related genes sensitize to CAP18

A chemogenomic screen revealed that LPS-related genes are highly enriched among gene overexpressions that sensitize to CAP18 but not to control peptide CP1 (p-values are FDR-adjusted values from two-sided Fisher's exact tests, n=3059); grey background denotes significant enrichments.

	CAP18		CP1	
	Odds ratio	**p-value**	**Odds ratio**	**p-value**
All LPS-related genes	3.21	3.40E-05	1.26	1.00
Lipid-A biosynthesis	4.40	0.004	2.04	0.47
Extracellular polysaccharide synthesis	0.78	1.00	2.17	1.00
LPS biosynthetic process	3.65	5.97E-05	0.18	0.64
LPS core region synthesis	2.63	0.54	0	1.00
LPS transport	0.00	1.00	NA	0.11
All phospholipid-related genes	2.31	1.00	3.65	0.52
Phospholipid transport	1.96	1.00	5.44	0.85
Phospholipid binding	5.24	0.49	4.35	1.00

Supplementary Table 12 – Combination Indices (CI) characterizing the antibiotic-PGLA interactions in the wild-type and corresponding antibiotic-resistant strains

The combination index for a given antibiotic and antimicrobial peptide pair was defined as the average of the combination index of the 7 antibiotic:antimicrobial peptide ratio. The cut-off values were CI≥1.14 for antagonism; CI≤0.86 for synergism; and 0.86<CI<1.14 for no interaction (for details see Materials and Methods). Relative combination index was calculated as the ratio between CIs in the resistant strain and corresponding wild-type strain for the same antibiotic-PGLA combination, so that Relative CI<1 represents induced synergism.

Antimicrobial peptide	AB	Wild-type strain	Resistant strain		Relative CI
		CI	Strain	CI	
PGLA	AMP	0.83	AMP2	0.35	0.42
			AMP6	0.56	0.67
			AMP8	0.51	0.61
	CHL	0.87	CHL2	0.47	0.54
			CHL7	0.62	0.71
	CPR	1.79	CPR7	0.56	0.31
			CPR9	0.44	0.25
	DOX	0.56	DOX1	0.26	0.45
			DOX3	0.26	0.46
	ERY	0.36	ERY1	0.36	1.00
			ERY8	0.30	0.85
	FOX	1.39	FOX1	0.54	0.39
			FOX7	0.57	0.41
	KAN	1.47	KAN8	1.63	1.11
			KAN6	2.25	1.53
	TET	0.93	TET3	0.33	0.35
			TET1	0.37	0.40
	TOB	1.43	TOB10	1.73	1.21
			TOB3	1.66	1.16
	TRM	1.08	TRM10	1.65	1.54
			TRM6	1.60	1.49

Supplementary Table 13 – Combination index (CI) values of PGLA–antibiotic (AB) combinations on *E. coli* clinical isolates and respective antibiotic-resistant strains

Provided in a separate Excel spreadsheet.

Supplementary Table 14 – Mutation-incorporating pORTMAGE oligonucleotides, allele-specific colony-PCR, HRM PCR and sequencing primers

Provided in a separate Excel spreadsheet.

Supplementary Figures

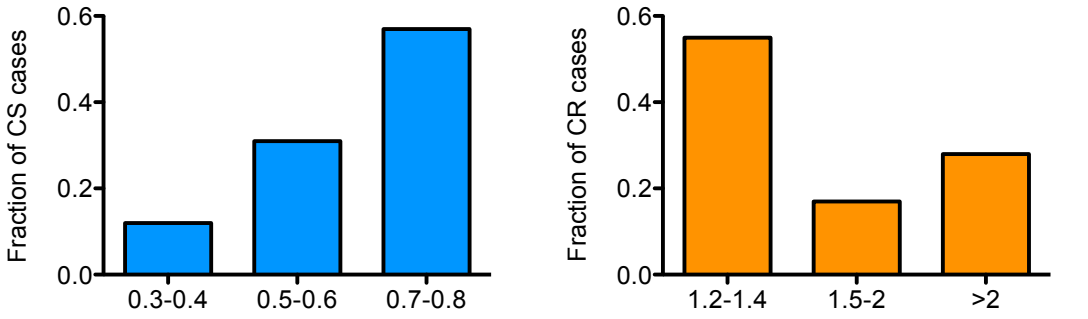

Supplementary Figure 1 - Distribution of the strength of collateral sensitivity (blue) and cross-resistance (orange) interactions

Abbreviation: MIC, minimum inhibitory concentration; CS, collateral sensitivity; CR, cross-resistance. Total sample size: CS n=49 strains and CR n=36 strains (Supplementary Table 4)

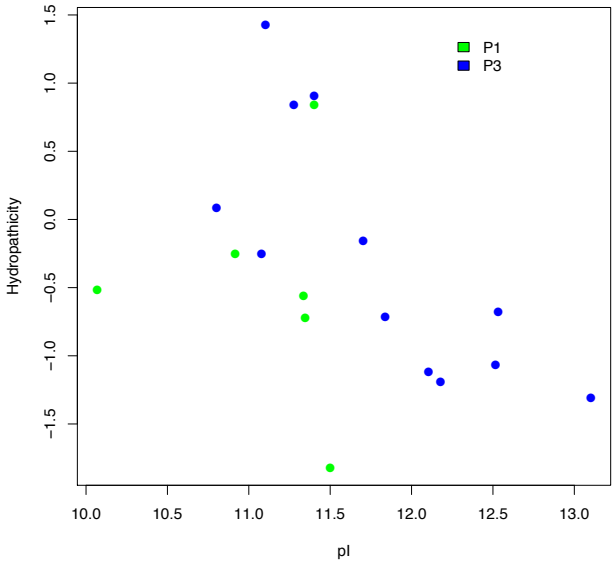

Supplementary Figure 2 - Hydropathicity and isoeletric point jointly separate the P1 and P3 peptide clusters

Antimicrobial peptides belonging to both P1 and P3 clusters generally insert themselves into membrane bilayers to form pores and thus induce cell lysis. However, the two groups differ in their collateral sensitivity profiles: while collateral-sensitivity is frequent towards P3 peptides, antibiotic-resistant strains rarely display either CS or CR interactions to P1 peptides. An analysis of the physicochemical properties (Supplementary Table 5) of peptides belonging to P1 (n=6) and P3 (n=12) clusters revealed that these peptides differ significantly when their isoelectric point and hydropathicity are considered together ($p = 0.018$, two-sided logistic regression, likelihood ratio test). These properties likely affect the peptides' behavior in aqueous solution and on the bacterial membrane surface, which could have a prominent effect on peptide-membrane interaction, especially in antibiotic-resistant strains with altered surface charge. As we could not identify any further biologically meaningful physicochemical properties that separate these two peptide clusters, we hypothesize that the difference in P1 and P3 cross-resistance and collateral sensitivity patterns could be the result of a combination of their differences in hydropathicity and isoelectric point.

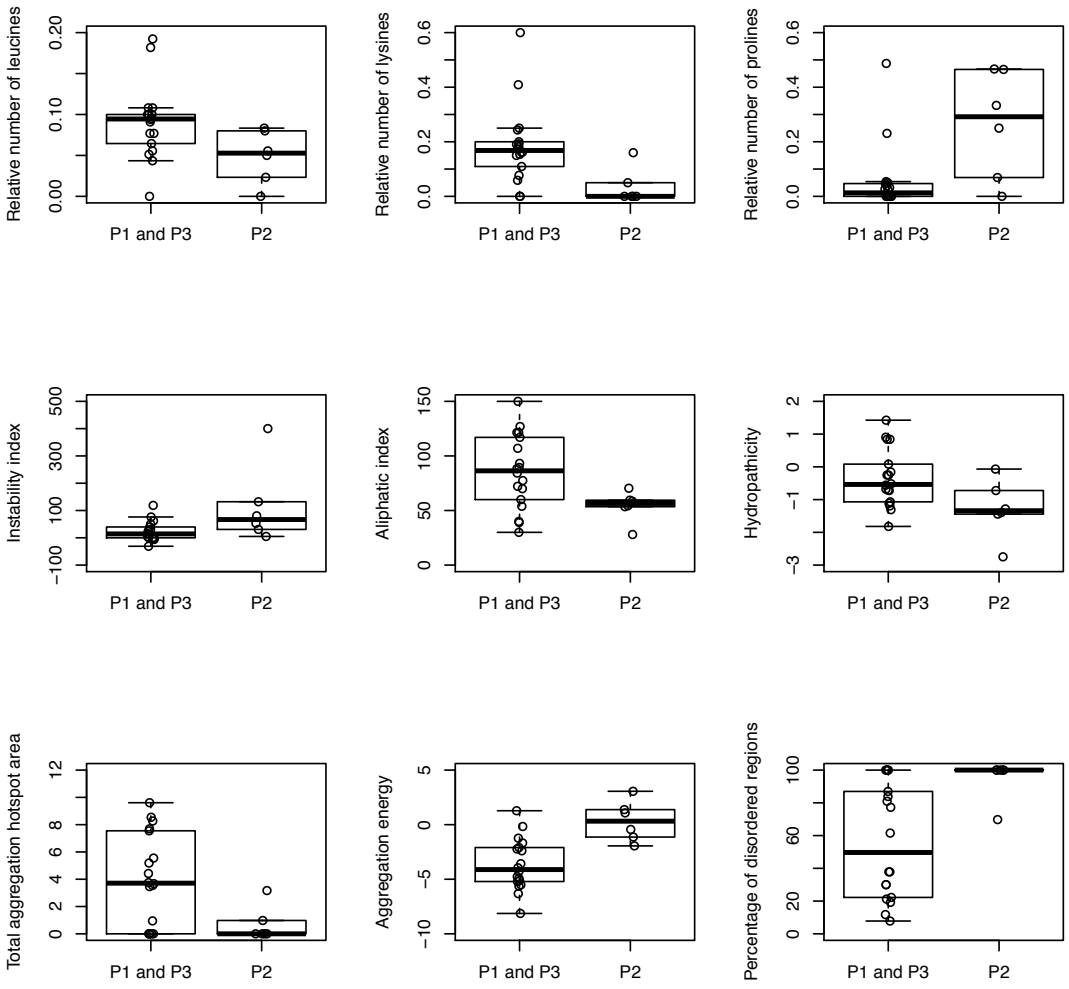

517

518 **Supplementary Figure 3 - Chemical and physical properties of the**
519 **peptides that differentiate P2 and P1/P3 antimicrobial peptide**
520 **groups**

521 The P2 peptide group (n=6) show significant differences ($p<0.05$ two-sided Wilcoxon
522 rank sum test) in the listed chemical properties from the P1 and P3 peptide groups
523 (n=18). P2 peptides consist of more proline, less lysine and leucine amino acids.
524 They are characterized by unstable secondary peptide structures; relatively low
525 aliphatic and hydropathicity indices, with smaller total aggregation-prone surfaces
526 and higher aggregation energies (for more details see Supplementary Table 5).
527 Boxplots present the median, first and third quartiles, with whiskers showing 1.5
528 times the interquartile range of the data.

529

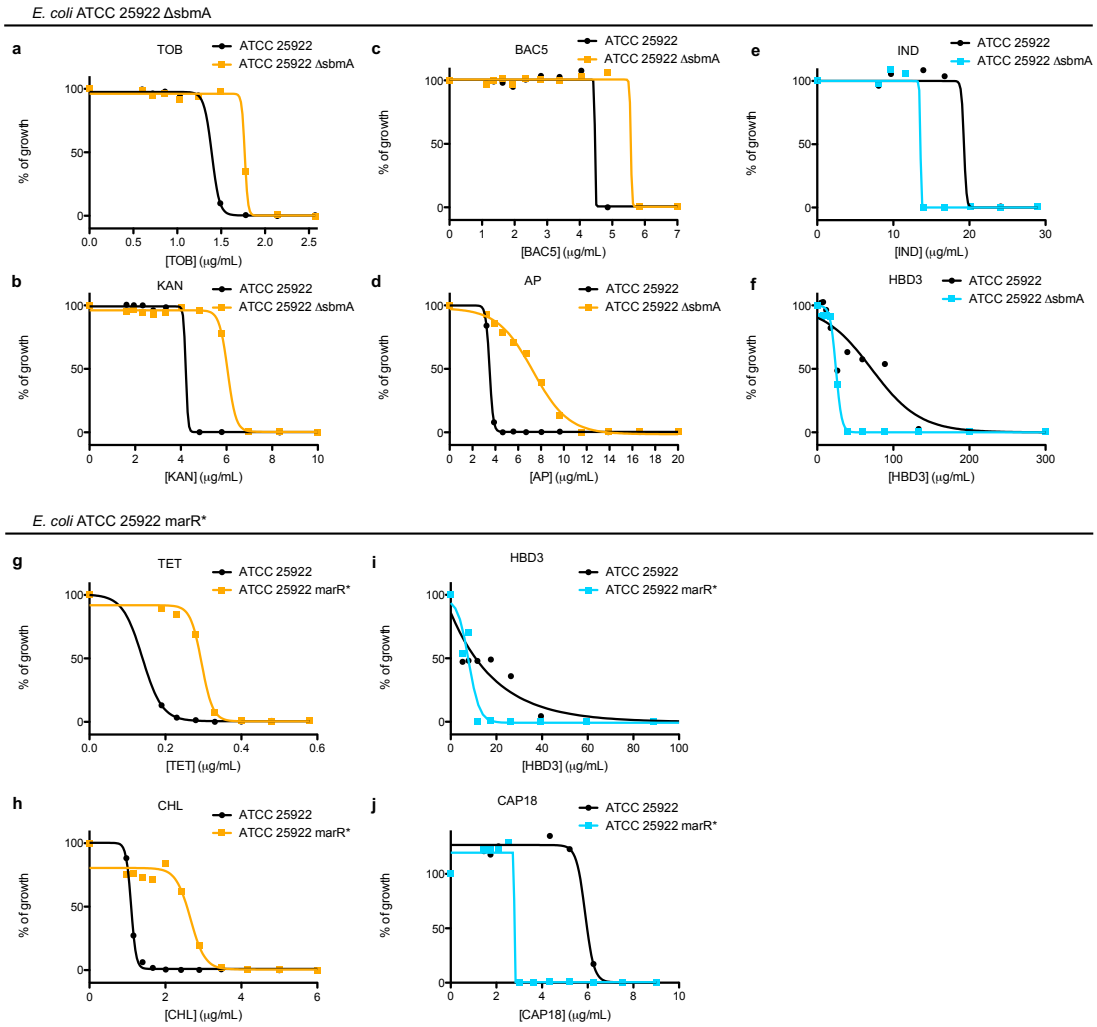

530

531 **Supplementary Figure 4 - Cross-resistance (orange) and collateral**
532 **sensitivity (blue) caused by resistant mutations in an antibiotic-**
533 **sensitive clinical isolate *E. coli* background**

534 Growth response curves of the clinical isolate *E. coli* ATCC 25922 strain (black) and
535 the same strain carrying the deletion of *sbmA* gene (upper panels **a**-**f**) or the
536 Val84Glu mutation in the *marR* gene (lower panels **g**-**j**), respectively. Cross-
537 resistance and collateral sensitivity patterns of these mutations in the clinical isolate
538 background are similar to those described in laboratory *E. coli* BW25133 (Table 1).
539 Specifically, deletion of *sbmA* provides low level of resistance to aminoglycosides
540 tobramycin (TOB) and kanamycin (KAN) as well as to proline-rich peptides
541 bactenecin 5 (BAC5) and apidaecin IB (AP). At the same time, the Val84Glu
542 mutation of the *marR* gene causes widespread cross-resistance to antibiotics like
543 tetracycline (TET) and chloramphenicol (CHL). Reassuringly, both mutations lead to
544 collateral sensitivity to P3 peptides (**e**, **f**, **i** and **j**) similarly to what we have observed

545 in *E. coli* BW25113. Data in this figure is representative of at least 2 biological
546 replicates.

547

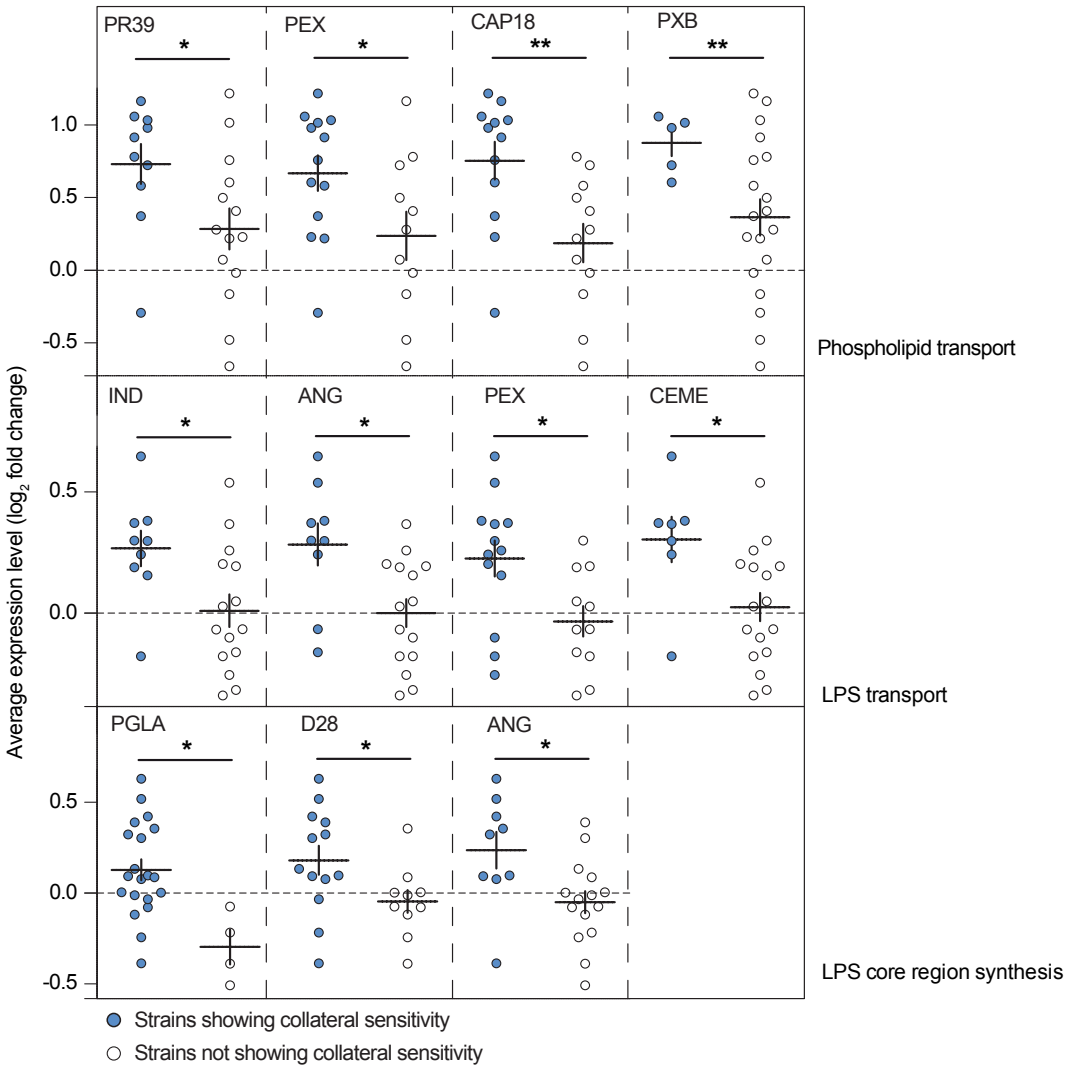

548

549 **Supplementary Figure 5 - Increased expression level in membrane-**
550 **related genes is associated with collateral sensitivity to**
551 **antimicrobial peptides**

552 Increased expression in membrane-associated genes is frequently observed in
553 antibiotic-resistant strains showing collateral sensitivity to a given antimicrobial
554 peptide compared to the rest of the strains (asterisks indicate p-values as follows:
555 0.001 < ** < 0.01 < * < 0.05, two-sided Student's t-tests). Scatter plots show the
556 mean with whiskers showing the standard error of the mean. The sample size of
557 each condition used in the analysis is provided in the Supplementary Table 3.

558

559

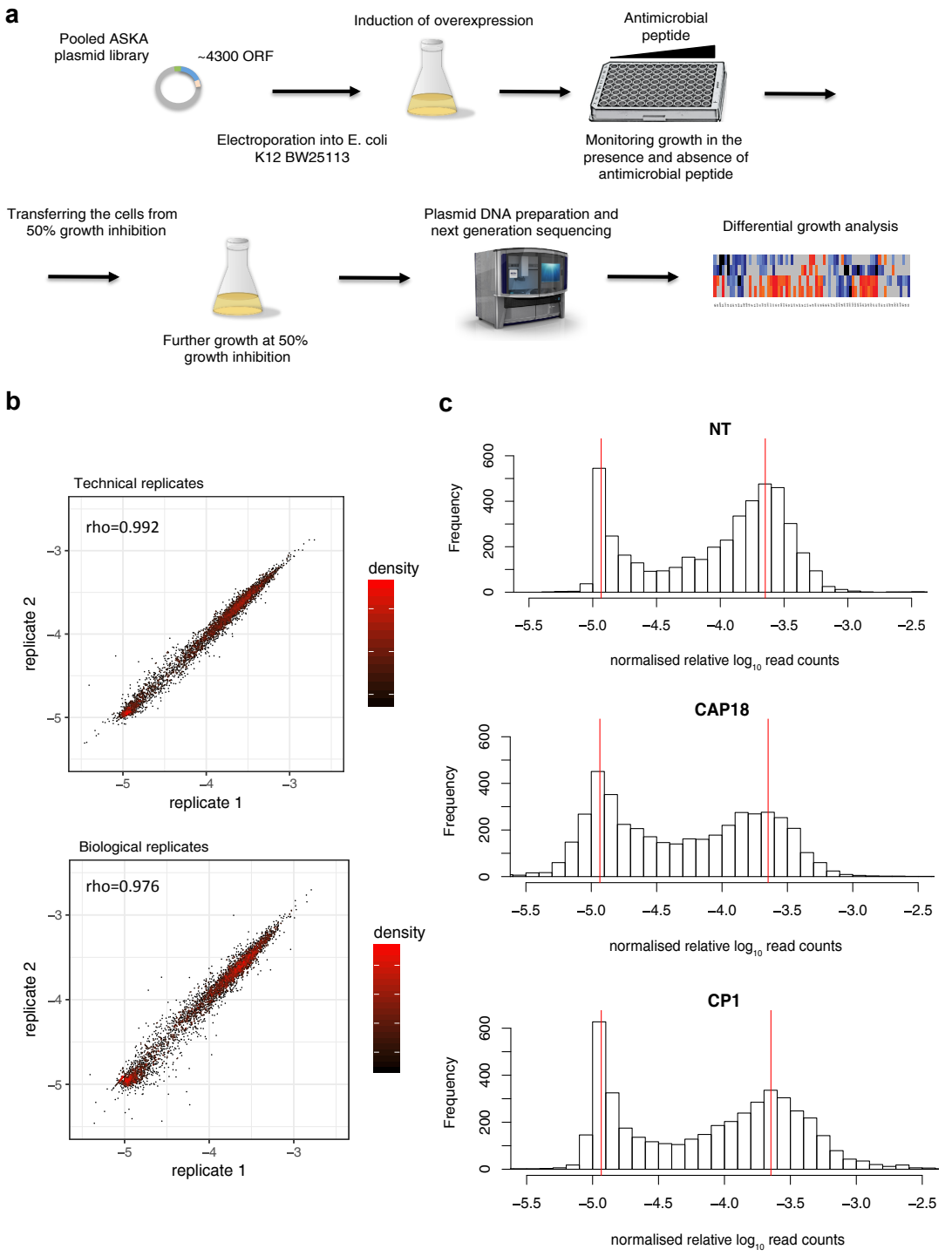

560

561 **Supplementary Figure 6 - Genome-wide chemogenomic screen**

562 **a,** The chemogenomic workflow applies a pooled fitness assay[26] with a deep
563 sequencing readout[27] to measure the interaction of gene overexpressions and
564 antimicrobial peptides on growth. To this aim, a pooled version of all *E. coli* ORF
565 overexpressing strain collection (ASKA collection) was grown in the absence and
566 presence of CAP18 and CP1, respectively, while mild overexpressions were induced

(for more details see Materials and Methods). Following approximately 12-15 generations of logaritmic growth, next-generation sequencing was applied on the resulting plasmid pool to measure the relative abundance of each overexpression strain in the populations. Analogously to a transcriptome analysis, the mapped read count of each ORF report on the abundance in the pooled sample, but in this competition assay the read counts are proportional to the frequency of each strain in the population. A relative drop in the abundance of a certain overexpression strain in the peptide-treated sample (differential growth analysis) indicates that the overexpressed gene sensitizes specifically in the presence of the antimicrobial peptide. **b,** Measurement noise in the competition experiments for the entire dataset (n=3059 genes). Technical replicates were generated on the same day, started from the same inoculum and sequenced together. Biological replicates were generated independently and sequenced separately. The data shows the distribution of the read counts mapped onto *E. coli* ORFs following loglinear transformation, but before normalization (see Materials and Methods). Pearson correlations between the replicates are indicated in the upper left corners. **c,** Distribution of the normalized read counts in the absence (NT) and presence of CAP18 or CP1. Following data processing (see Material and Methods), the distributions of the relative read counts show a bimodal distribution. The lower and upper modes correspond to ORFs that are not present in the sample anymore due to slow growth (indicated by the fact that this mode is close to loglinear(0) read counts even before normalization) and those that grow unaffected by the overexpression (indicated by the fact that this mode is close to loglinear(1/n) read counts, where n is the number of strains in the competition), respectively.

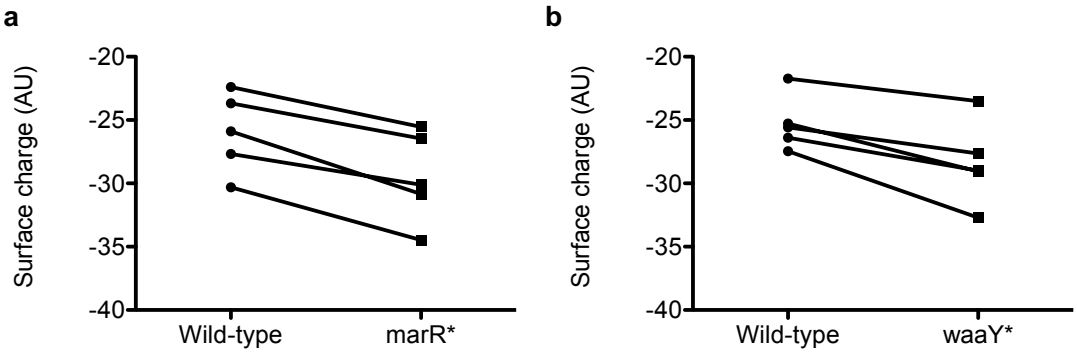

Supplementary Figure 7 - Cellular surface charge (zeta potential) of the *marR* single-mutant (marR*) and the *waaY* overexpressing strain (waaY plasmid)

Zeta potential of both *marR* (**a**) mutant and *waaY* (**b**) overexpressing strains, and the respective controls (see Materials and Methods). Both the *marR* mutant and the *waaY* overexpressing strain have a significantly increased negative surface charge (Two-sided paired t-tests p=0.0016 and p=0.0081, respectively). Comparisons are based on 5 biological and 8 technical replicates (i.e. each data point represents the average of 8 technical replicates). AU, arbitrary units.

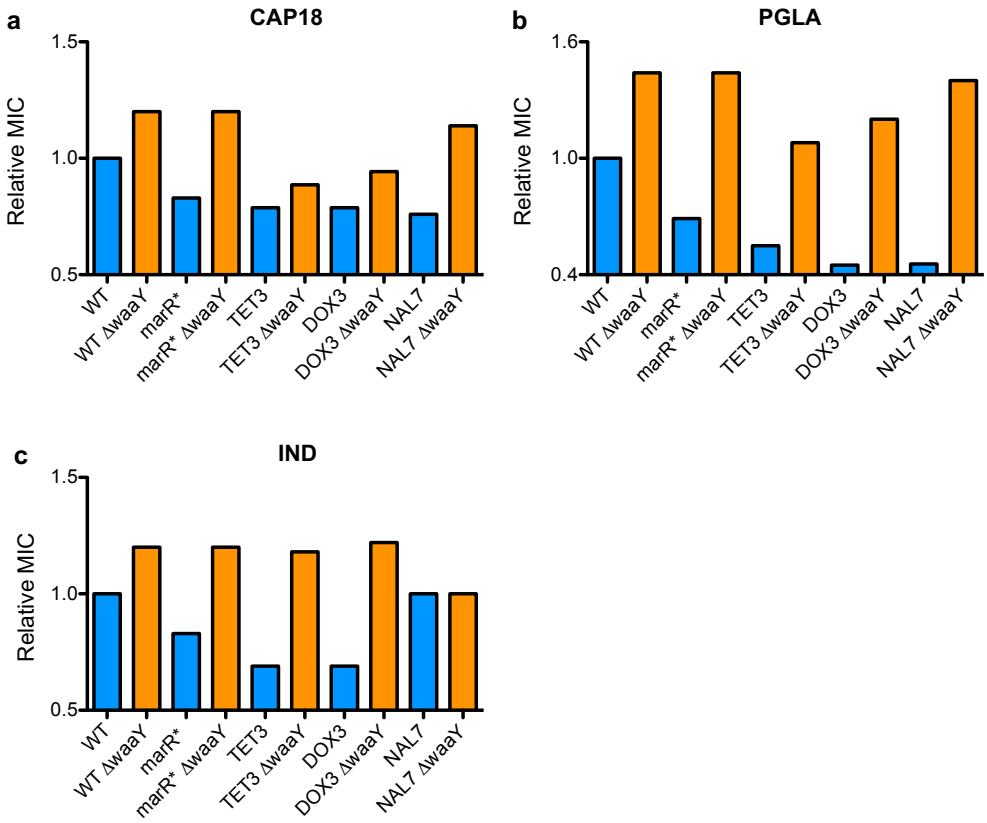

Supplementary Figure 8 - Inactivation of *waaY* in *marR* mutant strains leads to the loss of collateral sensitivity towards P3 peptides

The *marR* Val84Glu mutant (marR*) strain exhibits extensive collateral sensitivity to P3 peptides, such as CAP18, IND and PGLA (Table 1). We hypothesized that this mutation in the *marR* gene causes collateral sensitivity through upregulating the WaaY kinase responsible for phosphorylation of the inner core of lipopolysaccharides (LPS). To investigate the causal role of *waaY* in collateral sensitivity, we inactivated this gene in the wild-type *E. coli* BW25113 (WT) background, in the marR* mutant and in three antibiotic-resistant strains that carry a mutation in *marR* (TET3, DOX3 and NAL7) by inserting of two consecutive premature stop codons at the 10th amino acid position using pORTMAGE[2] (see Supplementary Method 4). Next, we measured the minimum inhibitory concentration of both the original (blue) and the waaY-inactivated (ΔwaaY, orange) strains towards P3 peptides, including CAP18 (**a**), PGLA (**b**) and IND (**c**). In agreement with data presented in Table 1, we observed collateral sensitivity of the marR* mutant and the antibiotic-resistant strains towards all three peptides, and no interaction of NAL7 strain towards IND. With the exception of this last example, the inactivation of *waaY* in the marR* mutant and in the

antibiotic-resistant strains not only led to the loss of collateral sensitivity, but in most cases also provided the same level of resistance as in the wild-type background. Please note that, with exception of TET3-CAP18, DOX3-CAP18 and NAL7-IND strain-peptide combinations, the extent of MIC increase in response to *waaY* inactivation was larger in the marR* mutant and antibiotic-resistant strains than in the wild-type. Relative MIC was calculated relative to the MIC of the wild-type (WT) for each of the strains. Data in this figure is representative of 2 biological replicates.

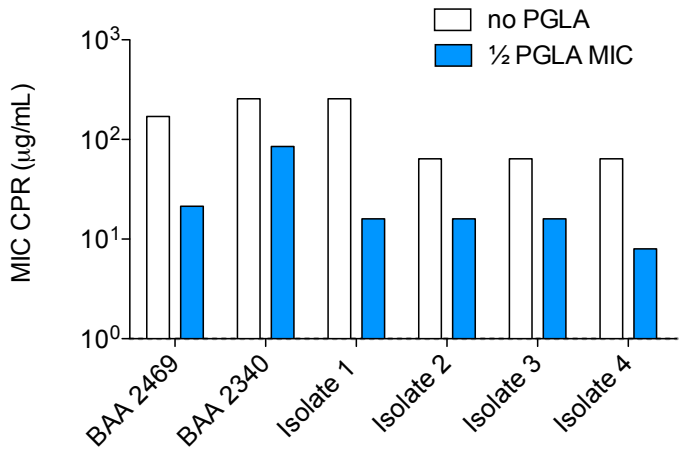

Supplementary Figure 9 - Impact of PGLA-ciprofloxacin cotreatment on resistance level in *Escherichia coli* clinical isolates

Ciprofloxacin (CPR) minimum inhibitory concentration (MIC) is shown on the y-axis on a logarithmic scale. The 6 ciprofloxacin-resistant *Escherichia coli* clinical isolates include two ATCC antibiotic-resistant reference strains (BAA 2469 and BAA 2340) and four strains (isolates 1 to 4) from a local hospital provided by the Department of Clinical Microbiology, University of Szeged, Hungary. Strains 1 to 3 were isolated from urine samples, while Strain 4 was isolated from intraperitoneal punction. CPR MICs were measured without (white) and with (blue) the presence of PGLA added at subinhibitory dosages (half of the MIC for each strain). We observed an approximately 4 to 16-fold decrease in ciprofloxacin MIC as a result of CPR-PGLA co-treatment in the six resistant strains. An antibiotic-sensitive reference strain (ATCC 25922) was also tested; the ciprofloxacin MIC of this strain remained the same: 0.008 μg/mL with or without PGLA. Data in this figure is representative of 2 biological replicates.

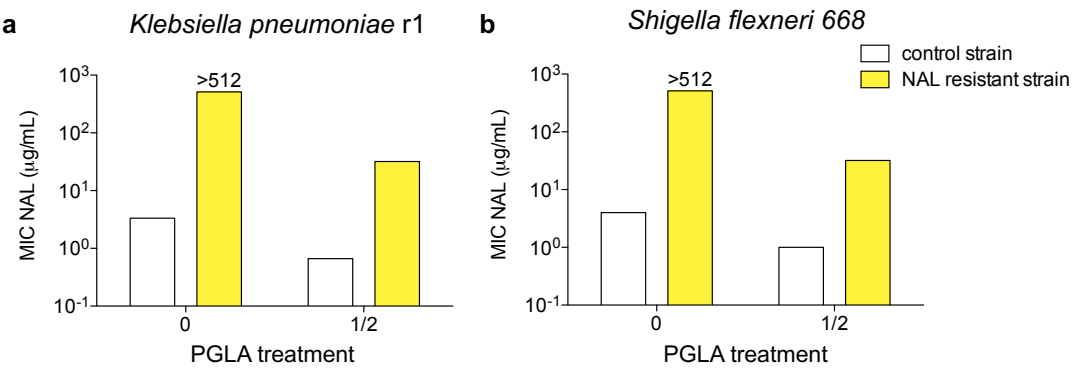

651

652 **Supplementary Figure 10 – Impact of PGLA–nalidixic acid co-**
653 **treatment on resistance level in *Klebsiella pneumoniae* and**
654 ***Shigella flexneri* strains**

655 To evaluate the efficiency of PGLA-Nalidixic acid co-treatment in pathogenic relatives
656 of *E. coli*, we tested how a subinhibitory concentration of PGLA affects the killing
657 efficiency of nalidixic acid (NAL) against NAL-resistant *Klebsiella pneumonia r1* (**a**)
658 and *Shigella flexneri* 668 strains (**b**), respectively. We observed an at least 16-fold
659 decrease in nalidixic acid MIC as a result of joint administration of PGLA in the
660 resistant strains and an approximately 4-fold decrease in the wild-type strains. As
661 previously (Supplementary Figure 9), PGLA was administered at subinhibitory
662 dosages. Naldixic acid sensitive (white) and resistant (yellow) *Klebsiella pneumoniae*
663 *r1* (**a**) and *Shigella flexneri* 668 (**b**) strains were provided by the Sommer lab (see
664 Materials and Methods). Nalidixic acid minimum inhibitory concentrations (MICs)
665 were measured without and with PGLA, at dosages around half of the peptide's MIC
666 for each strain tested. ">512" indicates an MIC value above the indicated value (no
667 exact values, due to the solubility limit of NAL above this concentration). Data in this
668 figure is representative of 3 biological replicates.

669

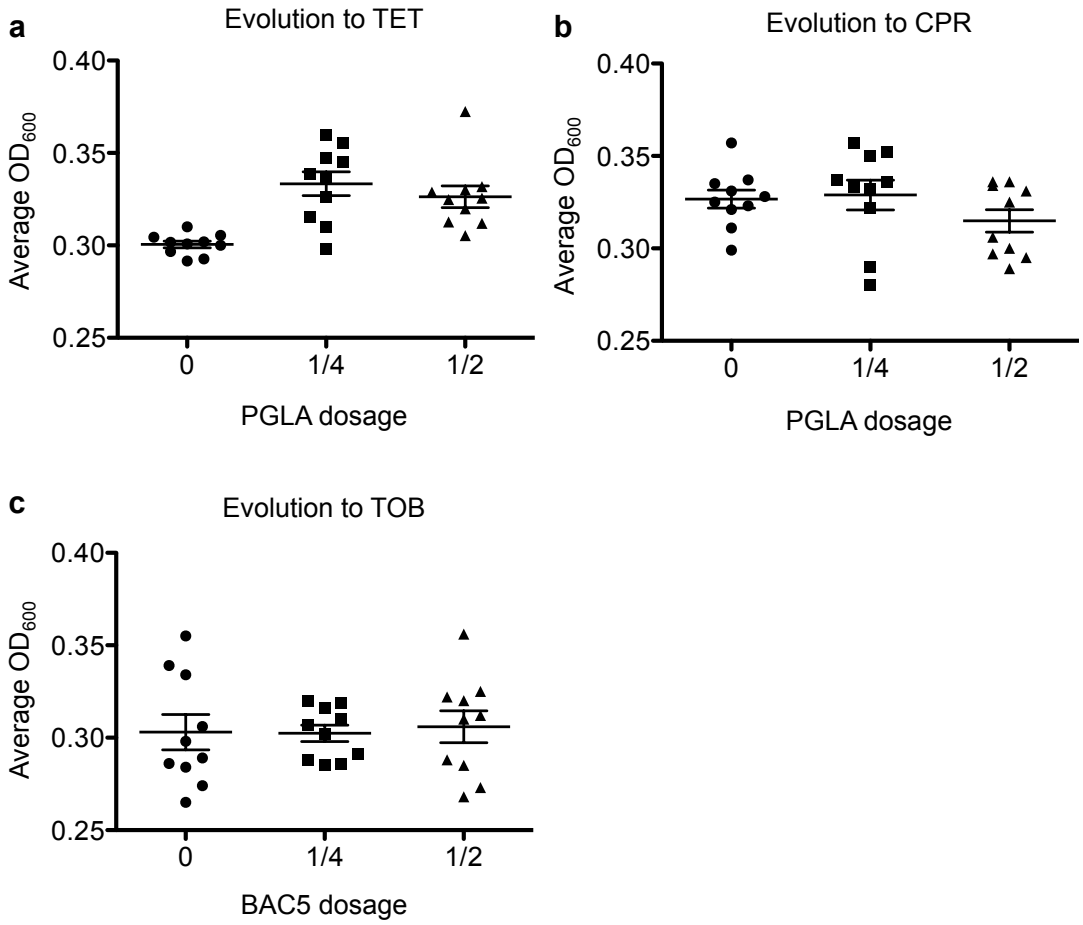

Supplementary Figure 11 – Population size of evolving lines throughout the evolutionary experiment

Population size was estimated by the optical density at 600nm (OD_{600}) of each parallel-evolved lines prior to each transfer. Ten parallel lines were subjected to laboratory evolution per each treatment. *E. coli* BW25113 was adapted to (**a**) tetracycline (TET), (**b**) ciprofloxacin (CPR), or to (**c**) tobramycin (TOB) in the presence and absence of PGLA/BAC5. 1/2 and 1/4 of the wild-type PGLA/BAC5 minimum inhibitory concentrations were employed. As a result of the protocol employed (see methods), the average OD600 during the course of the laboratory evolution was consistently between 0.3 and 0.35. We failed to find any significant decrease in population size as a result of antimicrobial peptide co-treatment. Scatter plots (n=10) show the mean with whiskers showing the standard error of the mean.

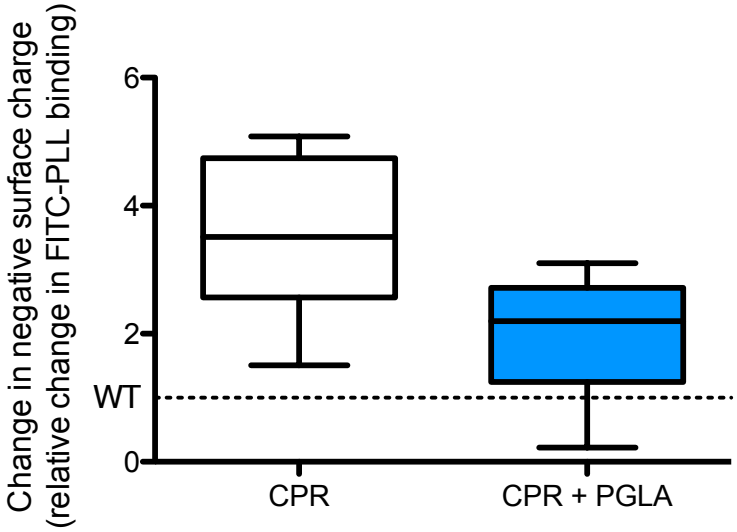

685

686 **Supplementary Figure 12 - Changes in cellular surface charge**
687 **upon adaptation to antibiotics in the absence and presence of a**
688 **subinhibitory dosage of PGLA**

689 We suspect that the efficiency of the antibiotic-PGLA co-treatment reflect elevated
690 costs of antibiotic resistance mutations under antibiotic-PGLA co-treatment. Because
691 CPR evolved lines show collateral sensitivity to PGLA, we speculate that such
692 mutations could cause changes in the bacterial membrane and therefore they would
693 be costly under CPR-PGLA co-treatment. As a preliminary test, we investigated the
694 changes in the cellular surface charge upon antibiotic adaptation in presence and
695 absence of PGLA. The purpose of this assay is to gain insight into the possible
696 mechanisms underlying the impact of PGLA-ciprofloxacin co-treatment on the *de*
697 *novo* evolution of ciprofloxacin resistance. In a nutshell, the surface charge of
698 laboratory-evolved bacteria was estimated using an established protocol[25] based on
699 FITC-labeled Poly-L-Lysine (FITC-PLL). Poly-L-lysine is a polycationic molecule
700 which is widely used to study the interaction between cationic peptides and charged
701 lipid bilayer membranes[24]. The binding assay was performed as described
702 previously[25]. The amount of bound FITC-PLL depends on the surface charge of the
703 bacterial cell. More bound FITC-PLL indicates a more negative surface charge[24,25].
704 The extent of change in negative surface charge was approximated by normalizing
705 FITC-PLL binding values of each evolved line to that of the wild-type. We focused on
706 laboratory lines independently evolved under ciprofloxacin (CPR) mono-treatment or
707 CPR-PGLA co-treatment, respectively (see main text and methods for details).
708 Reassuringly, we found that lines evolved under CPR mono-treatment exhibit an

increased negative surface charge compared to that of the wild-type (two-sided one-sample t-test, p=0.0001). Importantly, we found a significantly lower relative negative surface charge in lines evolved under CPR-PGLA co-treatment than those evolved under CPR mono-treatment (two-sided Mann-Whitney test, p=0.0040). At the same time, CPR-PGLA co-treatment leads to a substantially decreased level of resistance to both drugs (Figure 6, main text). Boxplots present the median, first and third quartiles, with whiskers showing the 5th and 95th percentile.

We hypothesize that this pattern reflects elevated costs of certain CPR resistance mutations under CPR-PGLA co-treatment. For instance, we established that certain mutations in *marR* increase resistance to CPR, but at the same increase susceptibility to PGLA, putatively via altering the cellular surface charge. A full answer to this question will require detailed molecular and phenotypic characterization of laboratory-evolved bacteria.

a

Strain	Relative MIC					
	TET	DOX	ERY	FOX	NAL	NIT
CAP18_2	1.00	0.36	0.26	0.83	0.40	0.83
CAP18_5	1.00	0.26	0.09	1.00	0.21	0.58
CAP18_6	0.83	0.58	0.19	1.20	0.46	0.69
CAP18_8	0.83	0.58	0.40	1.00	0.35	0.83
CAP18_10	1.96	1.00	0.58	2.25	0.35	0.40

Collateral sensitivity
No interaction
Cross-resistance

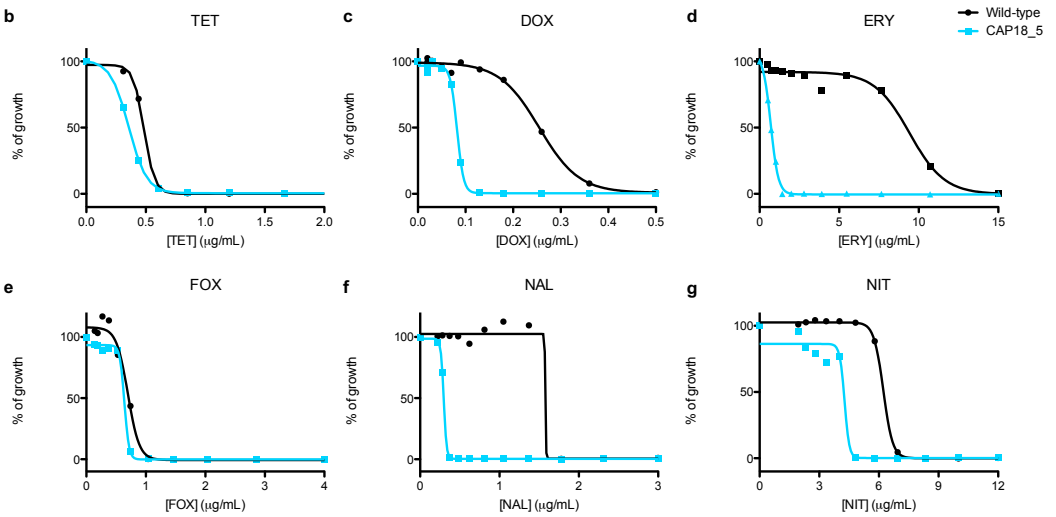

722

723 **Supplementary Figure 13 - Susceptibility of CAP18-resistant lines**
724 **towards a set of conventional antibiotics**

725 Susceptibility of five independently evolved CAP18-resistant strains was measured in
726 the form of minimum inhibitory concentration (MIC) towards six antibiotics, including
727 tetracycline (TET), doxycycline (DOX), erythromycin (ERY), cefoxitin (FOX), nalidixic
728 acid (NAL) and nitrofurantoin (NIT). Panel (**a**) shows the relative MIC values of all
729 five strains towards all six antibiotics compared to the wild-type. Relative MICs below
730 or above one indicate collateral sensitivity and cross-resistance, respectively. Panels
731 (**b**-**g**) show the detailed growth response curves for CAP18_5, as an example.
732 Growth response curves are representative of 2 biological replicates, while relative
733 MIC data in panel (**a**) is based on at least 2 biological replicates.

734

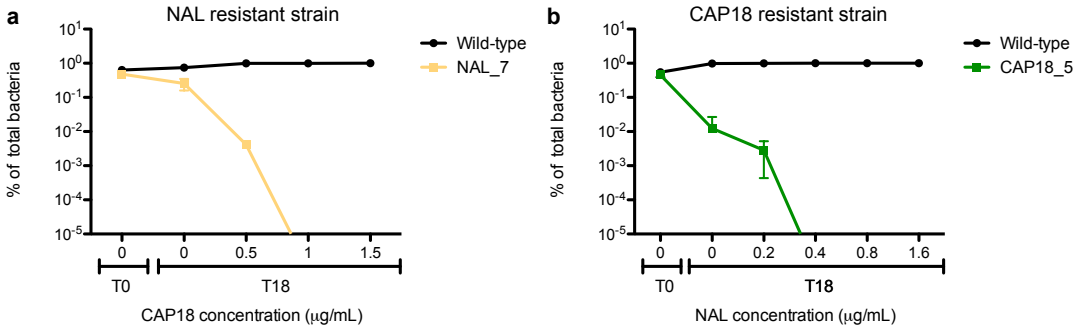

735

736 **Supplementary Figure 14 – Outcome of competition between drug-**
737 **resistant and wild-type strains.**

738 The figures show the ratio of resistant and wild-type bacteria competing in liquid
739 culture in the presence of different dosages of CAP18 (**a**) and naldixic acid (**b**),
740 respectively. At start (T0), the strains had equal frequencies (50-50%). After 18 hours
741 (T18), we observed a general decrease in the frequency of resistant bacteria,
742 demonstrating the existence of a concentration range where resistant bacteria can
743 be selectively eradicated. A relatively minor fitness cost of resistance was detected in
744 the absence of drug. Each data point shows the mean ± standard error of 3 biological
745 replicates. Colony forming units (CFU) were counted on agar plates. For further
746 details, see Supplementary Materials and Methods section.

747

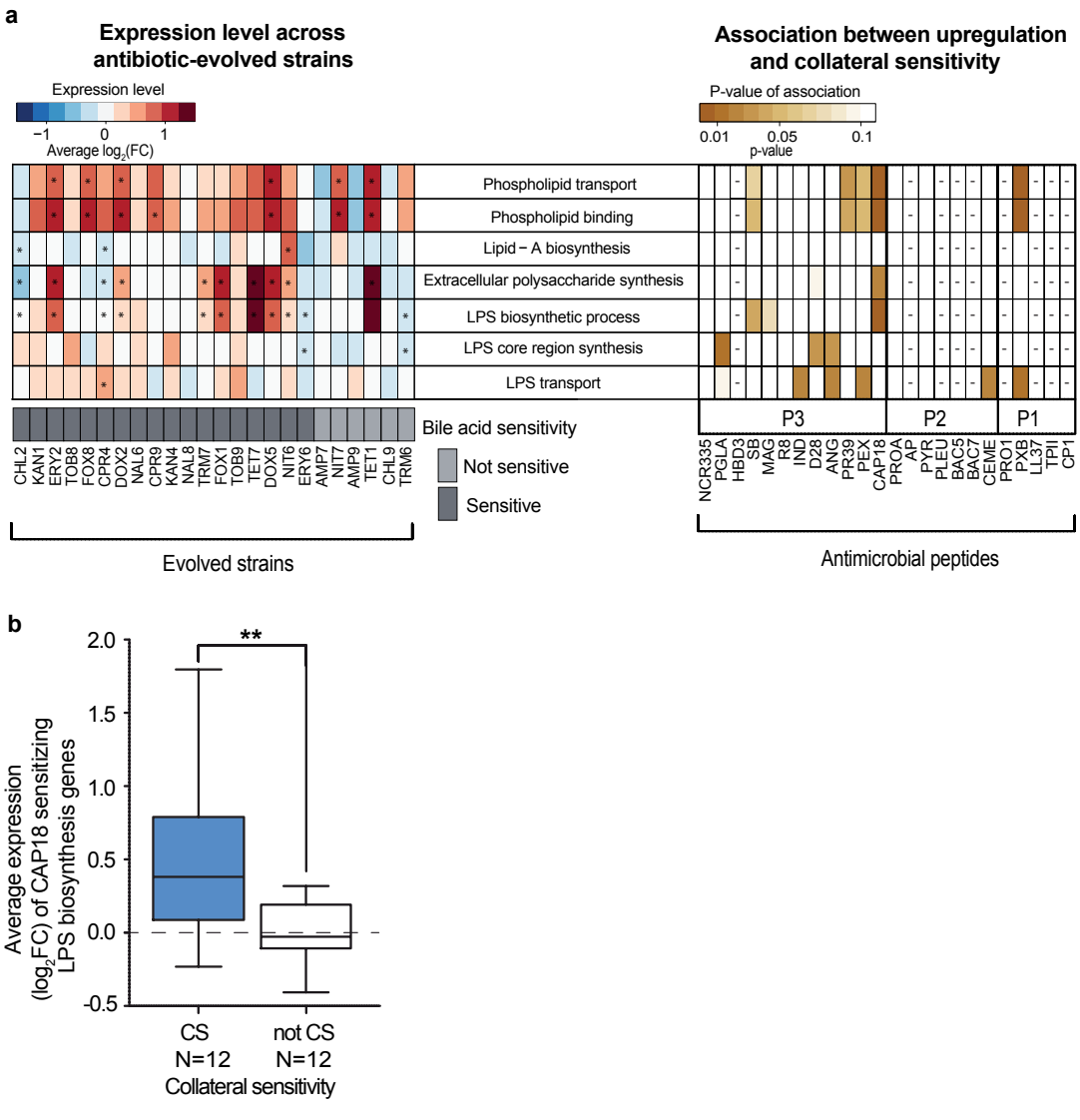

Supplementary Figure 15 - Altered membrane composition in antibiotic-resistant bacteria contributes to increased sensitivity to antimicrobial peptides when genes with stationary phase dependent expression were excluded

We carried out additional analyses to that of Figure 3 **c** and **d** to ensure that genes that tend to be differentially expressed in late growth phase do not confound our results. Such stationary phase regulated genes (N=449) were compiled from literature[28-30] and by identifying those genes in our dataset whose expression level was significantly correlated ($p<0.05$, Spearman's rho test) with OD at the time of sample collection in our experiments. Our conclusions remain after excluding genes with potential stationary phase dependent expression from our analyses. **a,** Left heatmap shows the average $\log_2$(fold change) of genes related to selected

761 membrane-associated GO processes and with no stationary phase dependent
762 expression. Many antibiotic-resistant strains are enriched in significantly up- or
763 downregulated genes (fold change>2 or <0.5, FDR-corrected p-value<0.05, two-
764 sided Fisher's exact test), associated with membrane-related functions. Significant
765 enrichments (p<0.05) are marked with an asterisk (*). Strains sensitive to a given
766 peptide show significant upregulations in specific GO groups compared to non-
767 sensitive strains (right heatmap, two-sided Student's t–test; for further details, see
768 Supplementary Figure 5). Peptides with either too few or too many collateral
769 sensitivity interactions (n<4 or n>21, respectively) were excluded from the statistical
770 analysis based on sample size calculation with alpha=0.1, power=0.8, delta=2,
771 SD=1, and are indicated with a minus sign (-). Sample size used in this analysis is
772 provided in Supplementary Table 3. **b,** Upregulation of LPS-related genes with no
773 stationary phase dependent expression sensitize to CAP18. CAP18-sensitive
774 antibiotic-resistant strains (CS, n=12) have significantly higher expression levels of
775 CAP18 sensitizing genes within the 'LPS biosynthetic process' GO category than
776 non-sensitive strains (not CS, n=12) (p=0.003, two-sided Wilcoxon rank-sum test).
777 Boxplots show the median, first and third quartiles, with whiskers showing the 5th
778 and 95th percentile. Significant difference (p<0.01) is marked with asterisks (**).

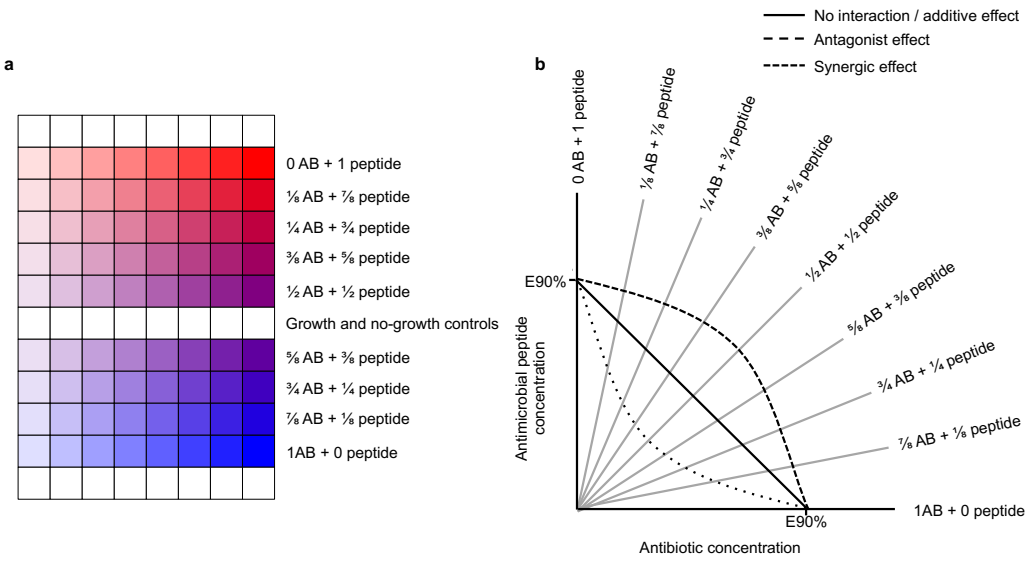

780 **Supplementary Figure 16 - Antibiotic-antimicrobial peptide**
781 **combination measurements: schematic representation of the plate**
782 **set up (a) and the combination assay (b).**

783 **a,** On each 96-well plate we probed the physiological interaction between one
784 antibiotic (AB, blue) and one antimicrobial peptide (red) as follows. We combined the
785 dilution series in 7 different antibiotic:peptide ratios. Thus, each plate contained 7
786 antibiotic:peptide ratio dilution series, dilution series of single agents, 4 bacteria-free
787 wells (no growth control) and 4 wells containing only medium without any drugs
788 (growth control). **b,** To calculate the combination index (CI) we first identified those
789 two concentration points for each antibiotic:peptide ratio where the inhibition of the
790 growth was 90% (EC90%). Then, by applying the Loewe additivity model to the
791 EC90% values of the single agents, we calculated the theoretical EC90% dosages
792 for each of the 7 antibiotic:peptide ratios. Geometrically, the theoretical EC90%
793 based on the Loewe model can be represented as a linear line between the EC90%
794 of the single agents in the two-dimensional linear concentration space. Deviation of
795 the shape of the lines connecting the experimentally measured EC90% from linearity
796 indicates either synergism (concave isoboles) or antagonism (convex isoboles).

797

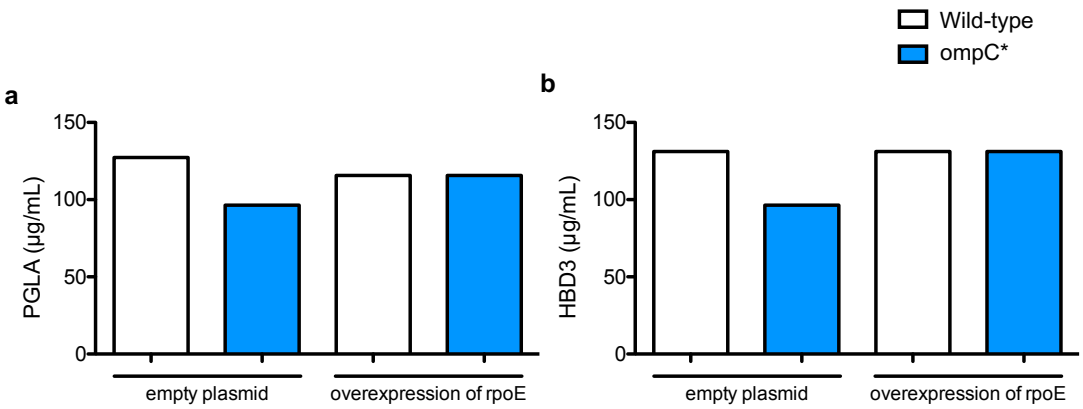

Supplementary Figure 17 - Overexpression of *rpoE* sigma factor eliminates collateral sensitivity of *ompC* loss-of function mutant

Strains carrying either a plasmid overexpressing the *rpoE* or an empty plasmid were established for both the wild-type and the *ompC* mutant strains (in all cases the plasmid was maintained by adding 10 ug/ml chloramphenicol and induced by 50nM IPTG). Minimum inhibitory concentration (MIC) was measured for PGLA (**a**) and HBD3 (**b**), to both of which the *ompC* mutant exhibited substantial collateral sensitivity. Data in this figure is representative of 3 biological replicates.

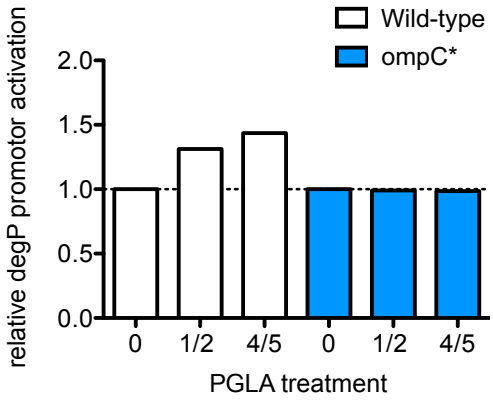

Supplementary Figure 18 - Sublethal dosages of PGLA leads to *degP* activation in the wild-type strain, but not in the *ompC* loss-of-function mutant

Both the wild-type strain and the *ompC* mutant were treated with either 50% (1/2) or 80% (4/5) of the PGLA peptide's minimum inhibitory concentration (MIC). Relative promoter activity was calculated by normalizing the measured promoter activity of each strain / condition to that of the untreated wild-type. Data in this figure is representative of 2 biological replicates.

References

1 Lázár, V. *et al.* Genome-wide analysis captures the determinants of the antibiotic cross-resistance interaction network. *Nat Commun* **5**, 4352, (2014).

2 Scocchi, M., Tossi, A. & Gennaro, R. Proline-rich antimicrobial peptides: converging to a non-lytic mechanism of action. *Cellular and Molecular Life Sciences* **68**, 2317-2330, (2011).

3 Pages, J.-M., James, C. E. & Winterhalter, M. The porin and the permeating antibiotic: a selective diffusion barrier in Gram-negative bacteria. *Nat Rev Micro* **6**, 893-903, (2008).

4 Fernández, L. & Hancock, R. E. W. Adaptive and Mutational Resistance: Role of Porins and Efflux Pumps in Drug Resistance. *Clinical Microbiology Reviews* **25**, 661-681, (2012).

5 Audrain, B. *et al.* Induction of the Cpx Envelope Stress Pathway Contributes to Escherichia coli Tolerance to Antimicrobial Peptides. *Applied and Environmental Microbiology* **79**, 7770-7779, (2013).

6 Mecsas, J., Rouviere, P. E., Erickson, J. W., Donohue, T. J. & Gross, C. A. The activity of sigma E, an Escherichia coli heat-inducible sigma-factor, is modulated by expression of outer membrane proteins. *Genes & Development* **7**, 2618-2628, (1993).

7 Mathur, J., Davis, B. M. & Waldor, M. K. Antimicrobial peptides activate the Vibrio choleraeσE regulon through an OmpU-dependent signalling pathway. *Molecular Microbiology* **63**, 848-858, (2007).

8 Egler, M., Grosse, C., Grass, G. & Nies, D. H. Role of the Extracytoplasmic Function Protein Family Sigma Factor RpoE in Metal Resistance of Escherichia coli. *Journal of Bacteriology* **187**, 2297-2307, (2005).

9 Crouch, M.-L. *et al.* The alternative sigma factor σE is required for resistance of Salmonella enterica serovar Typhimurium to anti-microbial peptides. *Molecular Microbiology* **56**, 789-799, (2005).

10 Ulvatne, H., Haukland, H. H., Samuelsen, Ø., Krämer, M. & Vorland, L. H. Proteases in Escherichia coli and Staphylococcus aureus confer reduced susceptibility to lactoferricin B. *Journal of Antimicrobial Chemotherapy* **50**, 461-467, (2002).

11 Weatherspoon-Griffin, N., Yang, D., Kong, W., Hua, Z. & Shi, Y. The CpxR/CpxA Two-component Regulatory System Up-regulates the Multidrug Resistance Cascade to Facilitate Escherichia coli Resistance to a Model Antimicrobial Peptide. *The Journal of Biological Chemistry* **289**, 32571-32582,

(2014).

12 Moffatt, J. H. *et al.* Colistin Resistance in Acinetobacter baumannii Is Mediated by Complete Loss of Lipopolysaccharide Production. *Antimicrobial Agents and Chemotherapy* **54**, 4971-4977, (2010).

13 Imamovic, L. & Sommer, M. O. Use of collateral sensitivity networks to design drug cycling protocols that avoid resistance development. *Sci Transl Med* **5**, 204ra132, (2013).

14 Jiao, Y. J., Baym, M., Veres, A. & Kishony, R. Population diversity jeopardizes the efficacy of antibiotic cycling. *bioRxiv*, (2016).

15 Lázár, V. *et al.* Bacterial evolution of antibiotic hypersensitivity. *Molecular Systems Biology* **9**, 700-700, (2013).

16 Zaslaver, A. *et al.* A comprehensive library of fluorescent transcriptional reporters for Escherichia coli. *Nat Meth* **3**, 623-628, (2006).

17 Bódi, Z. *et al.* Phenotypic heterogeneity promotes adaptive evolution. *PLOS Biology* **15**, e2000644, (2017).

18 Suzuki, S., Horinouchi, T. & Furusawa, C. Prediction of antibiotic resistance by gene expression profiles. *Nature Communications* **5**, 5792, (2014).

19 Nyerges, Á. *et al.* A highly precise and portable genome engineering method allows comparison of mutational effects across bacterial species. *Proceedings of the National Academy of Sciences* **113**, 2502-2507, (2016).

20 Minogue, T. D. *et al.* Complete Genome Assembly of Escherichia coli ATCC 25922, a Serotype O6 Reference Strain. *Genome Announcements* **2**, (2014).

21 Bonde, M. T. *et al.* MODEST: a web-based design tool for oligonucleotide-mediated genome engineering and recombineering. *Nucleic Acids Research* **42**, W408-W415, (2014).

22 Alves, C. S. *et al.* Escherichia coli cell surface perturbation and disruption induced by antimicrobial peptides BP100 and pepR. *J Biol Chem* **285**, 27536-27544, (2010).

23 Domingues, M. M., Santiago, P. S., Castanho, M. A. R. B. & Santos, N. C. What can light scattering spectroscopy do for membrane-active peptide studies? *Journal of Peptide Science* **14**, 394-400, (2008).

24 Rossetti, F. F. *et al.* Interaction of Poly(L-Lysine)-g-Poly(Ethylene Glycol) with Supported Phospholipid Bilayers. *Biophysical Journal* **87**, 1711-1721, (2004).

25 Peschel, A. *et al.* Inactivation of the dlt Operon inStaphylococcus aureus Confers Sensitivity to Defensins, Protegrins, and Other Antimicrobial Peptides. *Journal of Biological Chemistry* **274**, 8405-8410, (1999).

26 Pierce, S. E., Davis, R. W., Nislow, C. & Giaever, G. Genome-wide analysis of

barcoded Saccharomyces cerevisiae gene-deletion mutants in pooled cultures. *Nat. Protocols* **2**, 2958-2974, (2007).

27 Robinson, D. G., Chen, W., Storey, J. D. & Gresham, D. Design and Analysis of Bar-seq Experiments. *G3: Genes|Genomes|Genetics* **4**, 11-18, (2014).

28 Chang, D. E., Smalley, D. J. & Conway, T. Gene expression profiling of Escherichia coli growth transitions: an expanded stringent response model. *Molecular Microbiology* **45**, 289-306, (2002).

29 Tjaden, B. *et al.* Transcriptome analysis of Escherichia coli using high-density oligonucleotide probe arrays. *Nucleic Acids Research* **30**, 3732-3738, (2002).

30 Dong, T. & Schellhorn, H. E. Control of RpoS in global gene expression of Escherichia coli in minimal media. *Molecular Genetics and Genomics* **281**, 19-33, (2009).